Supplemental Information for

^{35}Cl - ^{1}H Heteronuclear Correlation MAS NMR Experiments for Probing Pharmaceutical Salts

Dinu Iuga, Emily K. Corlett, Steven P. Brown
Physics Department, University of Warwick, Coventry, CV4 7AL, UK

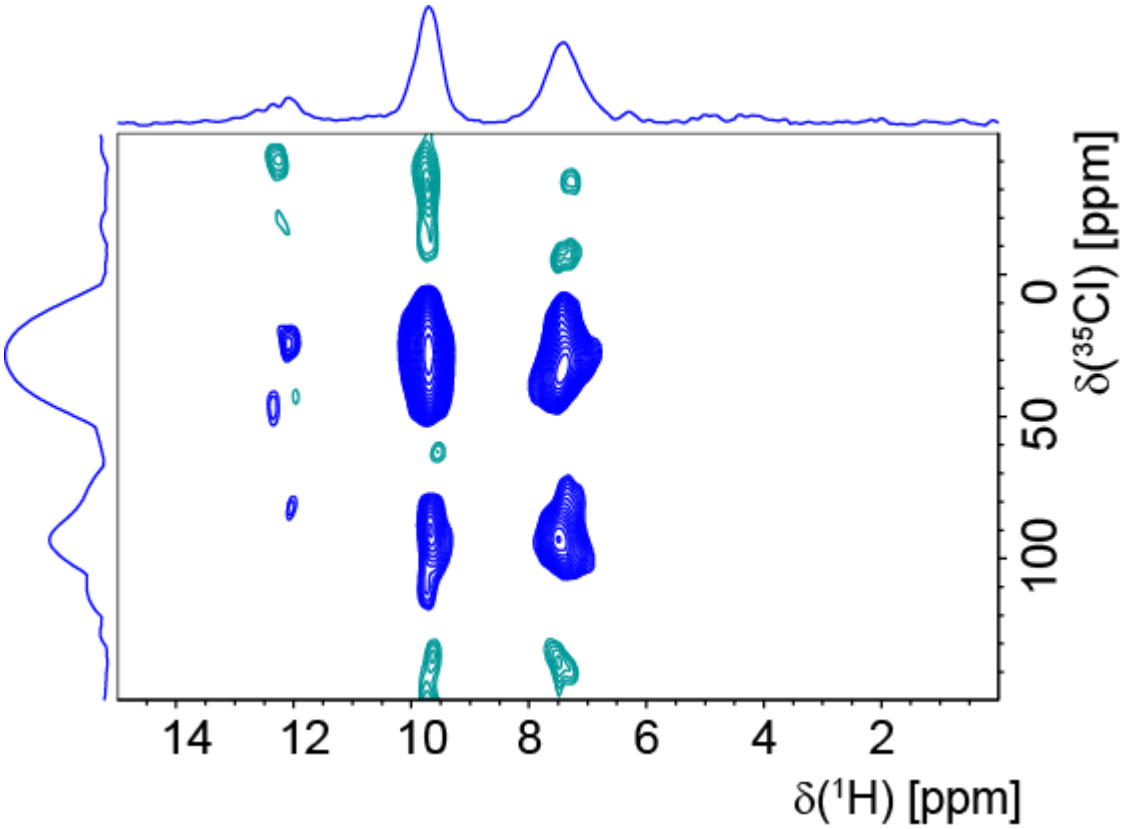

Figure S1 A ^{35}Cl – ^{1}H (850 MHz) D-HMQC MAS (60 kHz) NMR spectrum of L-tyrosine·HCl recorded with $\tau^{1}_{RCPL} = \tau^{2}_{RCPL}$ = 400 μs of phase-inverted R^{3} heteronuclear recoupling without WURST saturation of the ^{35}Cl satellite transitions (see pulse sequence diagram in Figure 1a). 128 transients were co-added for each of 100 rotor-synchronised t_1 FIDs with a 1 s recycle delay, corresponding to a total experimental time of 4 h. Positive and negative contours are shown in blue and green, respectively, with the base contour level at 15% of the maximum peak intensity.

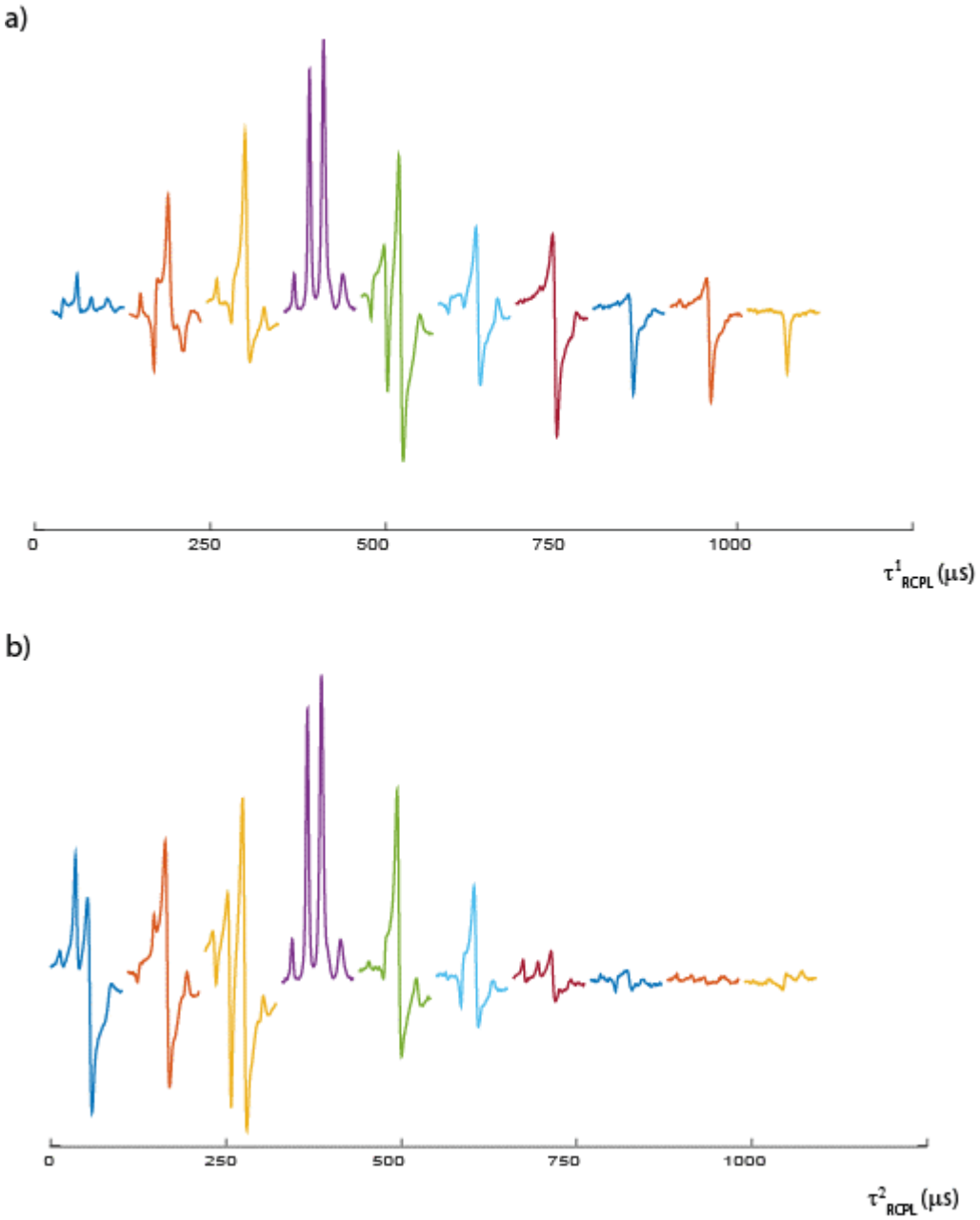

Figure S2 The dependence of signal intensity upon the recoupling time, a) τ^1_{RCPL} and b) τ^2_{RCPL} (with τ^2_{RCPL} and τ^1_{RCPL} set to 400 μs, respectively), for ^{35}Cl – ^{1}H (850 MHz) D-HMQC MAS (60 kHz) NMR experiments. The sum (over the ^{35}Cl dimension) for the ^{1}H spectral region from 1.0 to 11.2 ppm in the 2D correlation spectra is displayed, with the OH and NH_3^+ resonances at 9.7 ppm and 7.3 ppm, respectively. All 2D spectra used have the same phasing that is optimised for the $\tau^1_{RCPL} = \tau^2_{RCPL} = 400$ μs spectrum.

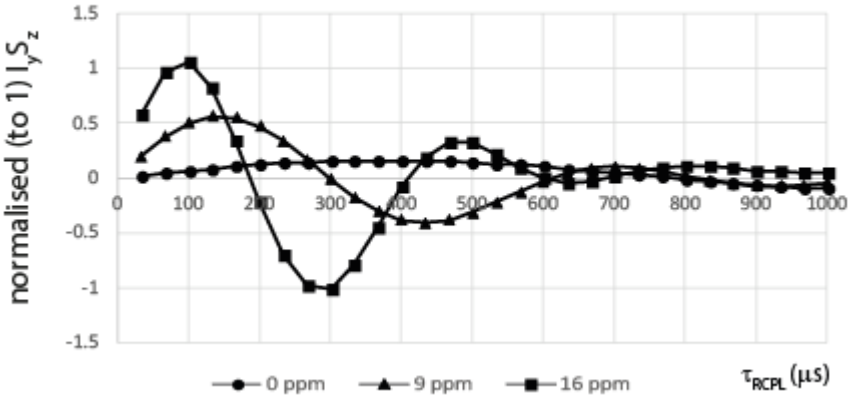

Figure S3 Simulated (SIMPSON) intensity of the $^{35}Cl - {}^{1}H$ (850 MHz) D-HMQC MAS (60 kHz) NMR experiment for one ^{35}Cl (with C_Q = 2.4 MHz and η = 0.72) and one ^{1}H for a dipolar coupling of 1.1 kHz starting from I_x coherence and monitoring evolution of the I_yS_z term for a ^{1}H CSA (with η = 0 and collinear principal axes system, PAS) of 0 ppm (circles), 9 ppm (triangles) and 16 ppm (squares).

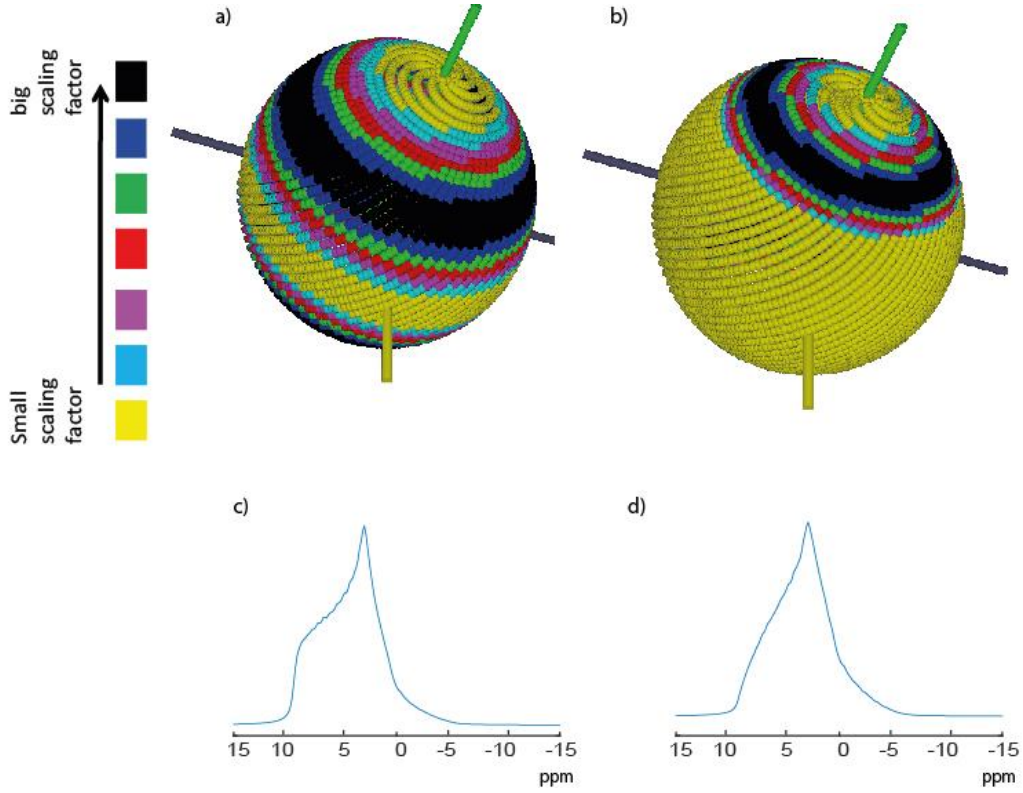

Figure S4 Colour coded distribution of the scaling factor for all orientations in a powder of ^{35}Cl nuclei coupled to a ^{1}H nucleus (with a dipolar coupling of 1.0 kHz, with the dipolar tensor having the same orientation as the quadrupolar tensor) after a) 33.3 μs and b) 1000 μs of $^{35}Cl - {}^{1}H$ $SR4^2_1$ recoupling The starting operator is I_x and the detect operator is I_yS_z. c) and d) Simulated lineshapes of the ^{35}Cl central transition if different orientation of the quadrupolar tensors are excited according to the scaling factors shown on a) and b) respectively.

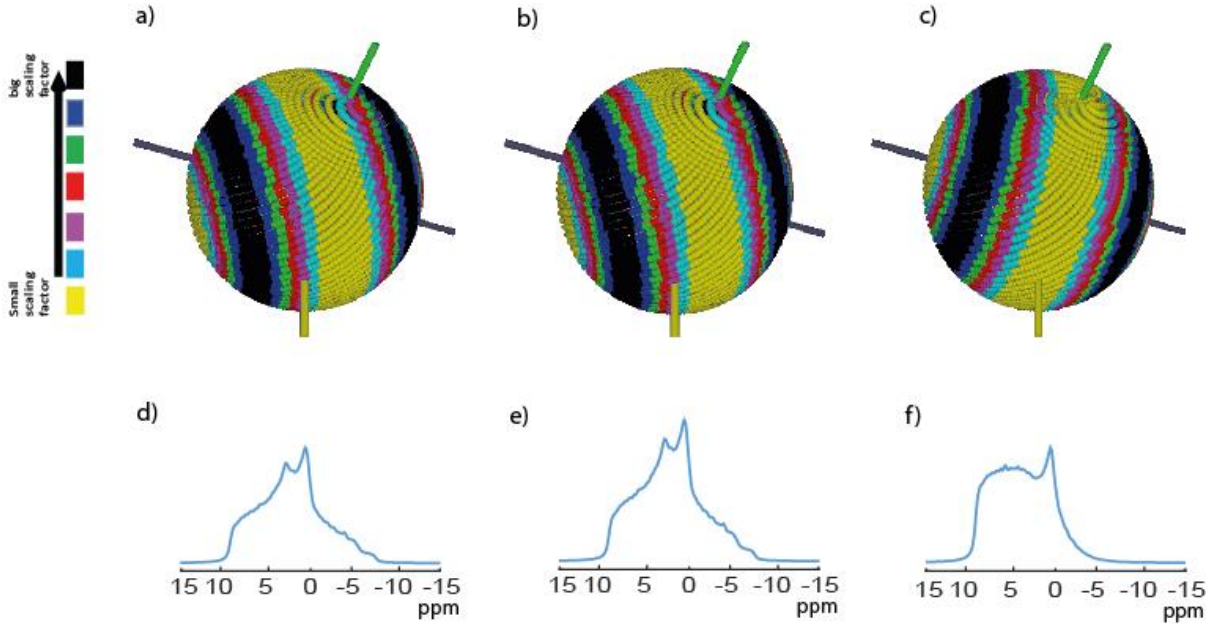

Figure S5 Colour coded distribution of the scaling factor for all orientations in a powder of a ^{35}Cl nucleus coupled to a ^{1}H nucleus with a dipolar coupling of 1 kHz, and with the dipolar tensor oriented at a) 30°, 70°, 20°, α, β, γ angles, respectively, for phase-inverted R^3 recoupling, b) 30°, 70°, 20°, α, β, γ angles, respectively, for $SR4^2_1$ recoupling, and c) 0°, 90°, 0°, α, β, γ angles, respectively, for $SR4^2_1$ recoupling. The starting operator is I_x, the detect operator is I_yS_z and the recoupling time is 33.3 μs. d), e) and f) Simulated lineshapes of the ^{35}Cl central transition if different orientation of the quadrupolar tensors are excited according to the scaling factors shown on a), b) and c) respectively.

S6. SIMPSON program to simulate a ^{35}Cl - ^{1}H 2-spin system undergoing $R4^2_1$ recoupling

```
spinsys {
channels 1H 35Cl
nuclei 1H 35Cl
shift 1 0 9p 0 0 0 0
dipole 1 2 -1000 0 0 0
quadrupole 2 2 2.40e6 0.72 0 0 0
}
par {
proton_frequency 850e6
spin_rate 60000
sw 10000
np 128
crystal_file zcw4180
gamma_angles 100
```

```
start_operator I1x
detect_operator I1y*I2z
verbose 1101
variable rf 120000
conjugate_fid false
}
proc pulseq {} {
global par
maxdt 1.0
set p90 [expr 0.25e6/$par(spin_rate)]
reset
pulse $p90 $par(rf) 90 0 0
pulse $p90 $par(rf) 270 0 0
pulse $p90 $par(rf) 90 0 0
pulse $p90 $par(rf) 270 0 0
pulse $p90 $par(rf) 270 0 0
pulse $p90 $par(rf) 90 0 0
pulse $p90 $par(rf) 270 0 0
pulse $p90 $par(rf) 90 0 0
store 1
reset
for {set i 0} {$i < $par(np)} {incr i} {
prop 1
acq
}
}
proc main {} {
global par

fsave [fsimpson] $par(name).fid
}
```

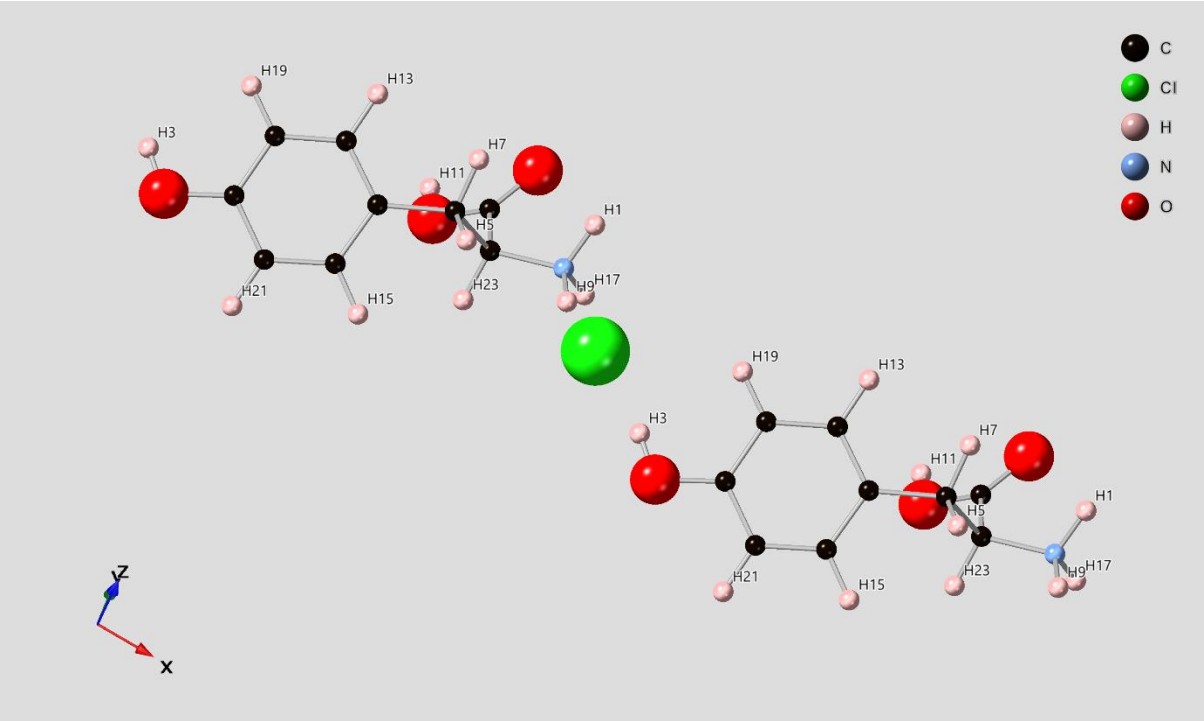

Figure S7 L-Tyrosine·HCl structure (after geometry-optimisation (CASTEP) of the CSD structure, LTYRHC10). The closest Cl-H (OH group) distance is 2.08 Å. For the NH_3^+ group, the Cl-H distances are 2.3, 2.4 and 2.5 Å.

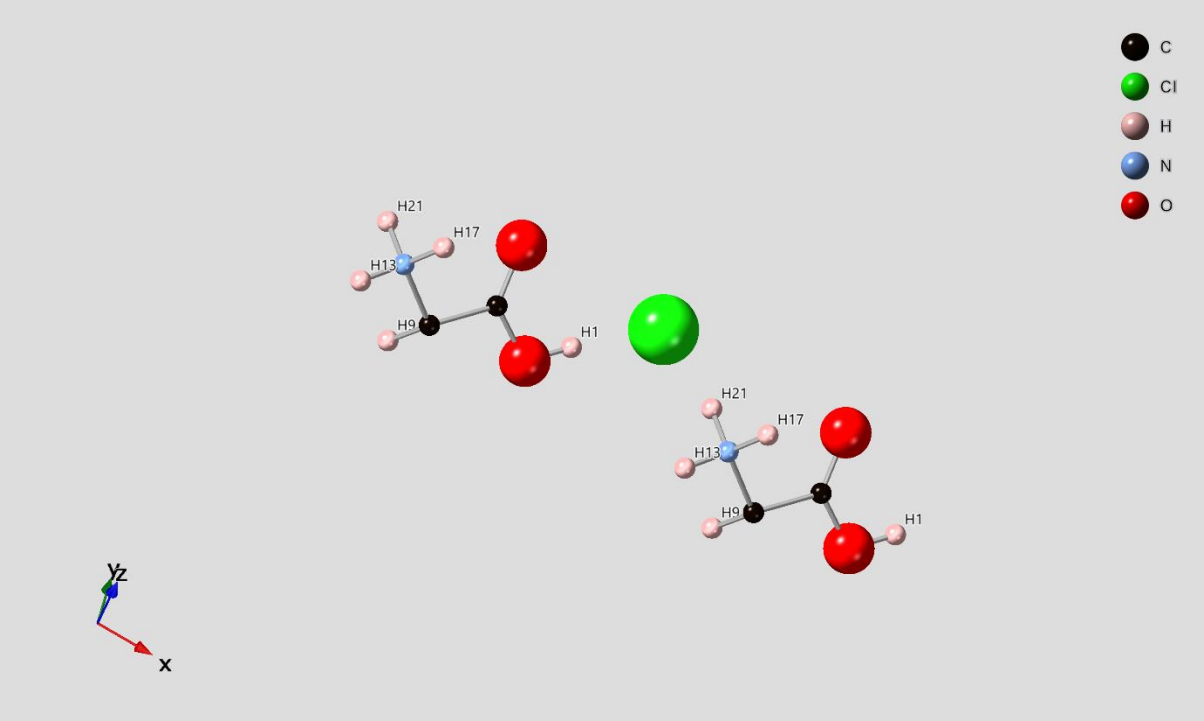

Figure S8 Glycine·HCl structure (after geometry-optimisation (CASTEP) of the CSD structure, GLYHCL01). The amine and the carboxylic acid protons are closest to the ^{35}Cl ion at 1.9 Å and 2.1 Å, respectively.

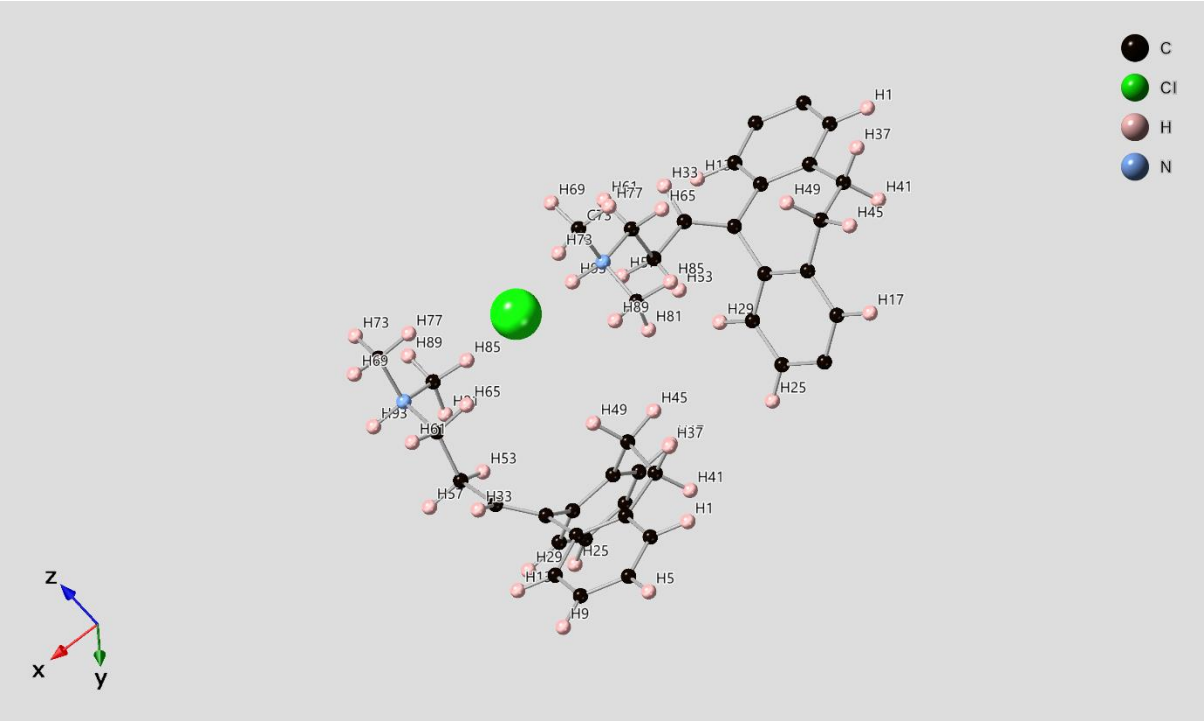

Figure S9 Amitriptyline·HCl (after geometry-optimisation (CASTEP) of the CSD structure, YOVZEO). The crystal structure indicates that the protons H93 at 11.3 ppm, H65 at 2.6 ppm and H89 at 2.8 ppm are closest to the ^{35}Cl ion at 1.9 Å, 2.7 Å and 2.7 Å, respectively.

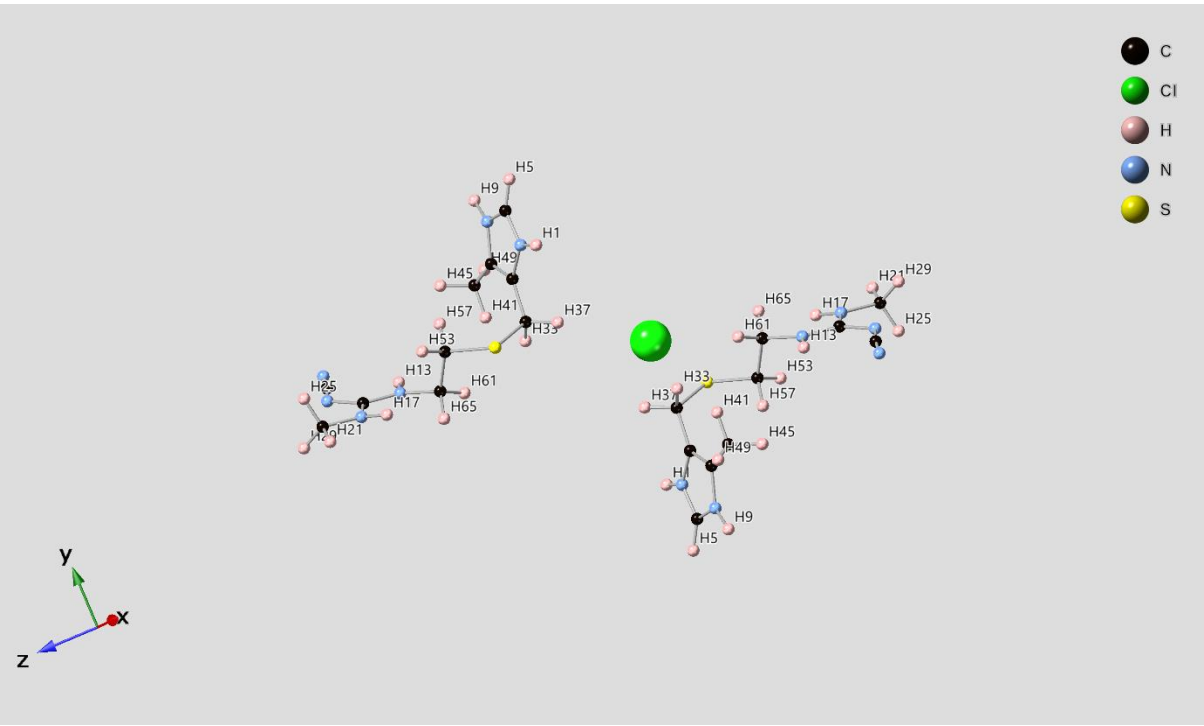

Figure S10 Cimetidine·HCl (after geometry-optimisation (CASTEP) of the CSD structure, EHIWEZ). The crystal structure indicates the protons H1 at 15.0 ppm, H9 at 15.1 ppm, H5 at 9.1 ppm and H33 at 4.0 ppm are at 2.0 Å and 2.6 Å and 2.8 Å away from the ^{35}Cl ion, respectively.

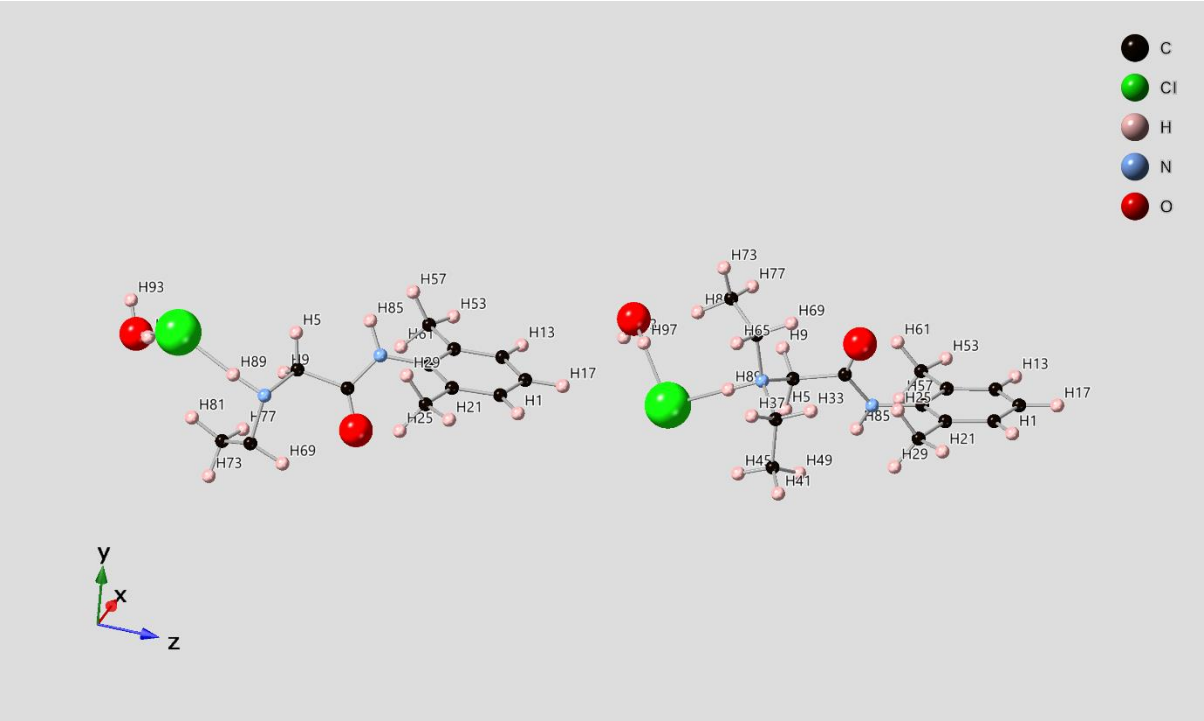

Figure S11 Lidocaine·HCl·H2O (after geometry-optimisation (CASTEP) of the CSD structure, LIDOCN01). The crystal structure indicates the protons H89 at 11.9 ppm, H97 at 4.3 ppm and H81 at 1.3 ppm are 2.0 Å, 2.2 Å and 2.9 Å, respectively away from ^{35}Cl.

Table S1: Experimental solid-state and GIPAW calculated ^{1}H NMR chemical shifts for L-tyrosine·HCl

Nucleus[a]	Calculated[b] δ_{ISO}/ppm	Experimental δ_{ISO}/ppm
H1	8.4	7.3
H3	10.6	9.7
H5	3.1	2.2
H7	2.0	2.2
H9	7.8	7.3
H11	13.6	12.2
H13	5.3	4.9
H15	7.1	6.4
H17	9.9	7.3
H19	6.1	4.9
H21	5.1	4.2
H23	3.3	2.2

[a] For atom labels, see Figure S1. [b] The reference shielding is 30.0 ppm

Table S2: Experimental solid-state and GIPAW calculated ^{1}H NMR chemical shifts for glycine·HCl

Nucleus[a]	Calculated[b] δ_{ISO}/ppm	Experimental δ_{ISO}/ppm
H1	13.0	11.8
H5	3.0	3.5
H9	4.2	3.5
H13	8.0	4.5

H17	6.3	4.5
H21	9.1	7.7

[a] For atom labels, see Figure S2. [b] The reference shielding is 30.0 ppm

Table S3: Experimental solid-state and GIPAW calculated ^{1}H NMR chemical shifts for amitriptyline·HCl

Nucleus[a]	Calculated[b] δ_{ISO}/ppm	Experimental δ_{ISO}/ppm
H1	6.2	6.8
H5	6.5	6.8
H9	5.5	5.8
H13	6.3	6.8
H17	6.5	6.8
H21	6.1	5.8
H25	5.3	5.8
H29	6.0	5.8
H33	5.4	5.8
H37	2.7	2.5
H41	2.4	2.5
H45	1.8	2.5
H49	3.2	2.5
H53	1.5	1.4
H57	1.8	2.5
H61	2.3	2.5
H65	2.6	2.5
H69	0.4	1.4
H73	0.9	1.4
H77	1.5	1.4
H81	1.5	1.4
H85	1.2	1.4
H89	2.8	2.5
H93	11.5	11.3

[a] For atom labels, see Figure S3. [b] The reference shielding is 30.0 ppm

Table S4: Experimental solid-state and GIPAW calculated ^{1}H NMR chemical shifts for cimetidine·HCl

Nucleus[a]	Calculated[b] δ_{ISO}/ppm	Experimental δ_{ISO}/ppm
H1	15.0	14.8
H5	9.2	9.1
H9	15.1	14.8
H13	4.4	4.8
H17	7.4	6.7
H21	0.9	2.2
H25	1.7	2.2
H29	1.9	2.7
H33	4.0	3.7
H37	3.6	3.7
H41	2.1	2.7
H45	1.8	2.2
H49	2.2	2.7

H53	2.2	2.7
H57	0.8	2.2
H61	2.5	3.7

[a] For atom labels, see Figure S4. [b] The reference shielding is 30.0 ppm

Table S5: Experimental solid-state and GIPAW calculated ^{1}H NMR chemical shifts for lidocaine·HCl·H2O

Nucleus[a]	Calculated[b] δ_{ISO}/ppm	Experimental δ_{ISO}/ppm
H1	6.3	5.2
H5	3.6	4.2
H9	3.4	4.2
H13	4.8	4.2
H17	6.8	7.0
H21	0.4	1.3
H25	1.1	1.3
H29	0.8	1.3
H33	2.3	1.3
H37	2.9	1.3
H41	0.7	1.3
H45	1.1	1.3
H49	0.8	1.3
H53	−0.8	1.3
H57	1.1	1.3
H61	1.0	1.3
H65	3.2	1.3
H69	3.7	1.3
H73	1.5	1.3
H77	1.5	1.3
H81	1.3	1.3
H85	10.9	10.4
H89	11.9	11.7
H93	3.9	4.2
H97	4.3	4.2

[a] For atom labels, see Figure S5. [b] The reference shielding is 30.0 ppm